Title

Retinoschisin gene therapy in photoreceptors, Müller glia or all retinal cells in the Rs1h−/− mouse

Journal

Gene Therapy, 21(6)

ISSN

0969-7128

Authors

Byrne, LC
Öztürk, BE
Lee, T
et al.

Publication Date

2014-06-01

DOI

10.1038/gt.2014.31

Peer reviewed

HHS Public Access

Author manuscript

Gene Ther. Author manuscript; available in PMC 2014 December 01.

Published in final edited form as:

Gene Ther. 2014 June ; 21(6): 585–592. doi:10.1038/gt.2014.31.

Retinoschisin gene therapy in photoreceptors, Müller glia, or all retinal cells in the *Rs1h−/−* mouse

Leah C. Byrne, PhD.[1,2], **Bilge E. Öztürk**[1], **Trevor Lee**[1], **Cécile Fortuny**[1], **Meike Visel**[1], **Deniz Dalkara, PhD.**[1,2,3], **David V. Schaffer, PhD.**[2], and **John G. Flannery, PhD.**[1,†]

[1]Department of Molecular and Cellular Biology and The Helen Wills Neuroscience Institute, The University of California, Berkeley, CA 94720

[2]Department of Chemical and Biomolecular Engineering, Department of Bioengineering, and The Helen Wills Neuroscience Institute, The University of California, Berkeley, CA 94720

Abstract

X-linked retinoschisis, a disease characterized by splitting of the retina, is caused by mutations in the retinoschisin gene, which encodes a secreted cell adhesion protein. Currently, there is no effective treatment for retinoschisis, though viral vector-mediated gene replacement therapies offer promise. We used intravitreal delivery of three different AAV vectors to target delivery of the RS1 gene to Müller glia, photoreceptors, or multiple cell types throughout the retina. Müller glia radially span the entire retina, are accessible from the vitreous, and remain intact throughout progression of the disease. However, photoreceptors, not glia, normally secrete retinoschisin. We compared the efficacy of rescue mediated by retinoschisin secretion from these specific subtypes of retinal cells in the *Rs1h−/−* mouse model of retinoschisis. Our results indicate that all three vectors deliver the RS1 gene, and that several cell types can secrete retinoschisin, leading to transport of the protein across the retina. The greatest long-term rescue was observed when photoreceptors produce retinoschisin. Similar rescue was observed with photoreceptor-specific or generalized expression, though photoreceptor secretion may contribute to rescue in the latter case. These results collectively point to the importance of cell targeting and appropriate vector choice in the success of retinal gene therapies.

Keywords

Gene therapy; X-linked retinoschisis; AAV vectors; photoreceptors; Müller glia; cell targeting

†Correspondence should be addressed to J.G.F. Address: University of California at Berkeley,132 Barker Hall, Berkeley, CA 94720-3190, Phone: (510) 642-0209, flannery@berkeley.edu.

[3]Current address: Institut de la Vision, UMRS 968 UPMC, INSERM, CNRS U7210, F-75012 Paris, France

Conflict of Interest

We disclose the following conflict of interest: DD, JGF, and DVS are patent holders on ShH10 for gene delivery to the retina. LB, DD, MV, JGF, and DVS are patent holders on 7m8 for delivery of gene products to retinal cells.

Introduction

X-linked retinoschisis (XLRS), which results from mutations in the gene encoding the secreted protein retinoschisin (RS1)[1], is a retinal degenerative disease affecting between 1/5,000 and 1/25,000 people worldwide[2–4]. The defining characteristics of XLRS include the formation of cystic cavities in the inner and outer retina and deterioration in vision caused by retinal disorganization.

The binding partners and molecular mechanism of retinoschisin have not yet been definitively characterized[5,6], though it is generally thought to be a cell adhesion protein. The mouse model of XLRS, which lacks the mouse homolog of retinoschisin, has a highly disorganized retina, mimicking the human condition, with formation of cavities and progressive loss of photoreceptors as a result of apoptosis that peaks 18 days after birth[7,8].

As the underlying cause of this recessive monogenic disease is well understood, it is an excellent candidate for gene augmentation therapy. Previous studies have shown that delivery of a normal copy of the RS1 gene using a variety of AAV vectors and routes of vector administration targeting a variety of cell types can ameliorate degeneration[9–16]. However, a direct comparison of the efficacy of rescue obtained via expression of RS1 from specific subsets of cells has not been conducted.

Recently, our group has created two novel variants of AAV that target specific populations of cells in the retina upon intravitreal injection. ShH10 is a variant of AAV6 that infects Müller glia specifically and efficiently[17,18], and7m8 is a variant of AAV2 that efficiently infects inner and outer retina[9]. While 7m8 infects cells throughout the retina, its transgene expression can be limited to rod photoreceptors using a rhodopsin promoter. Finally, both ShH10 and 7m8 mediate pan-retinal gene delivery following intravitreal administration, without a need for subretinal injection and accompanying retinal detachment.

Here, we evaluate structural and functional rescue following intravitreal injections of three different viral vectors targeting different subsets of retinal cells (Figure 1). Müller glia have been implicated in RS1 transport and normally provide structural support to retinal neurons. Müller cells have end feet that are easily accessible from the vitreous as well as processes reaching to the outer retina, and they remain intact in late stages of the disease. They may therefore be strong candidates to provide therapeutic protein, especially in later stages of the disease. In contrast, 7m8 with a rhodopsin promoter mediates protein expression specifically in photoreceptors. Since RS1 is strongly expressed by photoreceptors in normal retina, photoreceptors may be the best-suited cell type for delivering the protein. Lastly, 7m8 with a ubiquitous promoter transduces mixed populations of cells throughout the retina including ganglion cells, amacrine cells, Müller glia and photoreceptors.

We found expression of RS1 from photoreceptors to provide more effective long-lasting rescue than expression from Müller glia, with a similar rescue effect using a rhodopsin promoter or a ubiquitous promoter. These results suggest that the normal source of RS1 in the retina -- photoreceptors -- is optimal for processing and delivery of retinoschisin, as well as demonstrate the importance of vector selection and cell type targeting in the development of gene replacement therapies.

Results

Characterization of vector expression

The expression profiles of 7m8-rho, 7m8-CAG and ShH10-CAG following injection at P14 – into both WT and *Rs1h*−/− mice – were characterized using a GFP reporter and by immunolabeling of RS1 (Figure 2a–c). The expression profiles of the vectors were confirmed in WT and *Rs1h*−/− mice (Fig. 2a). 7m8 with a photoreceptor-specific rhodopsin promoter driving GFP led to photoreceptor-limited expression in the outer nuclear layer (ONL) in both WT and *Rs1h*−/− eyes. Additionally, 7m8-CAG-GFP targeted cells in all retinal layers, including ganglion, Müller, amacrine, photoreceptor and RPE cells. Finally, ShH10-CAG-GFP led to expression primarily in Müller cells in WT and *Rs1h*−/− retinas.

The distribution of secreted protein following injection of the vectors carrying cDNA for the human RS1 gene was evaluated by immunolabeling in WT and *Rs1h*−/− retinas (Fig. 2b). Labeling in eyes injected with 7m8-rho-RS1 showed high levels of RS1 protein in the retina, and a RS1 pattern localization comparable to WT indicated that the protein was transported to its natural target locations. Specifically, staining of RS1 was observed in photoreceptor inner segments, ONL, outer plexiform layer, inner plexiform layer and inner nuclear layer (INL). Injection of 7m8-CAG-RS1 resulted in strong RS1 labeling in photoreceptor inner segments, as well as inner retina, including in ganglion cells (white bordered inset). Finally, ShH10 led to significant production of the protein that was apparently transported from Müller cells in the inner retina to photoreceptors in the outer retina. In particular, photoreceptor inner segments were labeled with anti-RS1 antibody after ShH10 delivery, though the labeling at the inner segments was less intense than the staining observed in 7m8-rho-RS1 or 7m8-CAG-RS1 injected eyes. Co-labeling with an anti-glutamine synthetase (GS) antibody also showed RS1 protein on the surface of processes running parallel to Müller cells, which by their morphology and localization are likely bipolar cells. Intravitreal injection with each of three vectors thus produced strong panretinal retinoschisin expression with a distribution similar to wild-type.

To confirm secretion of RS1 from Müller cells, a western blot was performed on primary cultured Müller cells infected with ShH10-RS1 (Fig. 2c). RS1 was present in both Müller cell lysate and in the culture media, showing that Müller cells secrete RS1. In addition, a Western blot of retinas injected with the three vectors (3 retinas pooled for each condition) indicate similarly high levels of protein using all three vectors, comparable to the levels in a WT retina (Fig. 2d). In contrast, no retinoschisin protein was detectable in uninjected *Rs1h*−/− control eyes.

Time course of functional rescue

One important functional assessment of the XLRS retina is the electroretinogram (ERG), which records the change in the electrical potential of the retina in response to a flash of light. A decrease in the amplitude of the ERG b-wave with relative preservation of the a-wave is a hallmark of disorganization of the photoreceptor-bipolar cell synapse and reflectsa defect in synaptic transmission. To track functional rescue, the amplitude of the full-field scotopic electroretinogram b-wave was measured on a monthly basis after injection with all

three vectors (Fig. 3a). Administration of all three vectors led to an improvement in b-wave amplitude 1 month after injection relative to control GFP-injected or untreated eyes (7m8-CAG-RS1: 276±51 μV, 7m8-rho-RS1: 299±78 μV, ShH10-CAG-RS1: 274±51 μV, 7m8-GFP: 236±39 μV, untreated: 192±55μV). Over the course of four months, 7m8-CAG-RS1 and 7m8-rho-RS1 mediated significant and stable improvement in the b-wave amplitude compared to control eyes (7m8-rho-RS1 $P<0.0001$, 7m8-CAG-RS1, $P<0.001$, one-way ANOVA with post-hoc Tukey's multiple comparison test), while ShH10-mediated expression of RS1 from Müller glia led to a transient rescue effect at one month ($P<0.01$) that decreased over time. Four months after injection, amplitudes were 7m8-CAG-RS1: 291±14 μV, 7m8-rho-RS1: 297±47 μV, ShH10-CAG-RS1: 191±75 μV, 7m8-GFP: 137±15 μV, untreated: 171±75 μV. ShH10-CAG-RS1 n=5, 7m8-rho-RS1 n=8, 7m8-CAG-RS1 n=5. 7m8-rho-GFP n=8, untreated n=8. Representative ERG traces illustrate the amplitude of ERG recordings 4 months after injection (Fig. 3b).

ERGs were recorded from the same mice 4 months post-injection over a range of stimulus intensities under photopic (rod-saturating) and scotopic (dark-adapted) conditions (Fig. 3c). These recordings revealed that both 7m8-CAG-RS1 and 7m8-rho-RS1 led to rescue across the spectrum of light intensities tested, while ShH10-CAG-RS1 led to increases only at higher light intensities.

Because Müller glia often survive to later stages of retinal degeneration, we then tested the rescue potential of the three vectors using injections at a later time point. Injections made 30 days after birth also led to improvement of the amplitude of the scotopic b-wave when measured 4 months post-injection (Fig. 3d), though injection with 7m8-CAG-RS1 (n=5, 251±27 μV, $P<0.05$) and 7m8-rho-RS1 (n=5, 250± 36 μV $P<0.05$) led to greater rescue than ShH10 (n=5, 221±18 μV, not significantly different from GFP-treated eyes: 175±5 μV). Statistical significance was determined using a using a one-way ANOVA with posthoc Tukey's multiple comparison. Rescue with all three vectors was reduced with injection at this later time point relative to the P14 administration.

Structural improvement

High-resolution spectral domain optical coherence tomography (SD-OCT) images of retinas were gathered four months post-injection to evaluate the structure of the retina. Untreated eyes or control eyes treated with 7m8-GFP were marked by large cavities across the retina, (Fig. 4), whereas retinas treated with 7m8-rho-RS1, and 7m8-CAG-RS1 had fewer cavities and improved retinal organization. Treated retinas were thinner than WT retinas of the same age, with decreased ONL thickness, indicative of loss of photoreceptors. ShH10-CAG-RS1 retinas appeared similar to untreated eyes, though some improvement was noted in individual cases.

Long-term structural rescue

SD-OCT was used to determine the longevity of benefits on retinal structure following injection with 7m8. Imaging was performed on animals injected with 7m8-rho-RS1 and 7m8-rho-GFP in the contralateral eye. Ten months post-injection with 7m8-rho-RS1, OCT images indicated improved thickness of the retina in RS1 injected eyes and improved retinal

organization in inferior and superior quadrants of the retina (Fig. 5a). Quantification of thickness of retinal layers showed improved thickness of the retina, primarily in the ONL and photoreceptor inner and outer segments (Fig. 5b).

Histology in aged mice

Immunolabeling was used to determine the benefits of gene replacement on the integrity of the photoreceptor-bipolar cell synapse in aged animals (Fig. 6a). Specifically, retinas from animals injected at P14 were collected 15 months post-injection and labeled with anti-synaptophysin antibodies (a presynaptic marker labeling synaptic vesicles). The presence of synaptophysin labeling in the outer plexiform layer indicates synaptic transmission at the photoreceptor-bipolar cell synapse. In WT mice, dense labeling of synaptophysin at the photoreceptor-bipolar cell synapse was observed (arrowhead). In contrast, *Rs1h*−/− retinas were largely deficient of synaptophysin 15 months after birth, and control, 7m8-rho-GFP injected eyes were unchanged compared to untreated eyes. In contrast, 7m8-rho-RS1 injected eyes had dense labeling of synaptophysin. These retinas were also thicker, with a clear improvement of synaptic structure and retinal organization. Finally, ShH10-CAG-RS1 retinas were not significantly improved.

Over time, *Rs1h*−/− mice lose photoreceptors. PNA labeling of flatmounted retinas from 15 month-old animals showed increased densities of cones in 7m8-rho-RS1-treated eyes compared to untreated, GFP-injected or ShH10-injected eyes (Fig. 6b). Imaris software was used to count individual cones in PNA-labeled flatmounts.10X images were collected from the periphery of the retina and centered on the optic nerve head. Quantification of cones showed higher numbers of cones in animals treated with 7m8-rho-RS1, but not with ShH10.

Long-term functional rescue

The long-term functional benefit of 7m8-rho-RS1 was determined by ERG recordings collected 15 months after injection. At this late time point, 7m8-rho-RS1 injected eyes were significantly improved over control contralateral eyes expressing GFP or ShH10-CAG-RS1-injected eyes (7m8-rho-RS1: 161.4±29 μV; ShH10-CAG-RS1: 71.33 ±30.57 μV; 7m8-rho-GFP: 10.0±6 μV; P=0.0008) (Fig. 6c). Representative ERG waveforms illustrate higher amplitude of the a- and b-waves as well as a well-maintained wave form in treated eyes (Fig 6d).

Discussion

XLRS is a well-characterized monogenic inherited retinal degenerative disease and represents a promising candidate for gene replacement immediately amenable to the clinic. Recent clinical trials for LCA2 have proven the safety of AAV vector administration in the eye, though the invasive subretinal injections used in LCA2 may not be suitable for structurally compromised retinas. For example, XLRS is characterized by the formation of cystic cavities in the inner and outer layers of the retina and an increased risk for retinal detachment, and subretinal injections may therefore represent surgical risks in these fragile retinas. Additionally, subretinal injections transduce only a fraction of the retina. Retinoschisin is a secreted protein that may diffuse to a certain degree laterally across the

retina, though in a larger human eye the extent of this diffusion is uncertain, and RS1 gene therapy would likely require several injections to fully treat the condition. The ideal vector, therefore, should transduce the optimal cell type pan-retinally via an intravitreal injection. Previous studies in the mouse model of XLRS demonstrated that the disease is amenable to gene therapy[9,10,13,15], though significant hurdles exist in translating these studies to clinical use.

Here we tested a Müller glia-targeted approach to deliver RS1 to the *Rs1h*−/− retina as previous studies have suggested that Müller glia are involved in the transport of the protein to the inner retina[19,20]. In addition, we hypothesized Müller cells could provide advantages for a gene therapy approach due to their morphology, location and relative preservation in late stage retinal degeneration. In areas with large cavities, Müller glia may bridge schisis in the retina to deliver protein to the inner retina after photoreceptors have lost contact with the inner retina. However, our results showed that Müller cell-mediated expression was suboptimal for achieving rescue in the retinoschisin mouse model, demonstrably less effective than expression from photoreceptors. This suggests that if Müller cells are normally involved in RS1 trafficking, this mechanism alone is insufficient for normal retinal function. Our results show that Müller cells are able to express and secrete RS1, resulting in distribution of the protein throughout the retina, but must lack the ability for some other necessary aspect of processing or delivery of the protein to its molecular targets. It would therefore be necessary to understand and overcome these shortcomings in order for Müller cell-targeted RS1 delivery to be an adjunctive to photoreceptor-based therapy for RS1 gene replacement.

It is thus surprising that the rescue effect with ShH10 was less than that of 7m8-rho-RS1, although the onset of expression, pattern of localization and expression levels of RS1 protein are similar to WT in the ShH10-RS1 treated mice. This may indicate that Müller cells are unable to efficiently traffic RS1 to its binding partners, which recent studies show include the Na/K-ATPase subunits ATP1A3 and ATP1B2[21]. While photoreceptors express both of these subunits strongly, Müller glia do not express ATP1A3[22]. A lack of the normal binding partners of RS1 in Müller cells could thus affect the stability or processing of the protein. Future work should evaluate possible differences in the stability, trafficking, post-translational modifications and isoforms of RS1 secreted from Müller glia and photoreceptors.

In contrast, we have shown previously[9] and here that 7m8-rho-RS1, which mediates expression specifically in rods, rescues the morphology of the *Rs1h*−/− retina and thereby leads to long-lasting structural and functional preservation. This agrees with previous studies demonstrating that subretinal injections of AAV-mouse opsin promoter-RS1 mediated strong rescue through targeting photoreceptors[15].

All retinal neurons express RS1 during development, with a wave of expression moving outward starting at P1 in ganglion cells, proceeding to bipolar cells, followed by photoreceptor expression by P7[23]. In addition, ganglion cells have been reported to express RS1 into adulthood[23]. We therefore tested whether simultaneous expression from all cell types in the retina would increase the rescue effect of gene replacement. We found that

expression from multiple cell types afforded no measurable improvement over expression exclusively in rods (using the rhodopsin promoter), indicating that photoreceptor expression is sufficient for effective rescue when injections are made at P14. Additional benefit from ubiquitous expression may only be observed in the *Rs1h*−/− mouse model if injections are made early enough for RS1 protein to be expressed during retinal development, when retinoschisin is expressed strongly in a wave of expression in other cell types. However, anterograde transport of some AAV serotypes has been observed[24], and therefore a photoreceptor-specific promoter may represent a safer approach to gene augmentation therapy.

None of the vectors tested prevented the photoreceptor loss that peaks at P18, which occurs soon after the injections made at P14, likely due to the fact that gene expression takes several days to initiate and is thus not sufficiently rapid to avert this early wave of apoptosis. However, in humans the rate of degeneration in XLRS is much slower than in the murine model[3], and the therapeutic window for gene replacement treatments is longer.

In summary, this work indicates the importance of a rational approach to the design of gene replacement therapies and evaluation of the strategies used for viral vector-mediated delivery, including the cell type targeted and the delivery method. These results emphasize the potential for gene therapy in XLRS, highlighting the importance of careful design and optimization for specific, minimally invasive and long-lasting gene therapy.

Materials &Methods

Production of viral vectors

AAV vectors carrying human RS1 cDNA or GFP were produced by the plasmid co-transfection method [25]. Recombinant AAV was purified by iodixanol gradient ultra centrifugation followed by a buffer exchange and concentration with Amicon Ultra-15 Centrifugal Filter Units in PBS + 0.001% Pluronic F-68. Titers were determined by quantitative PCR relative to a standard curve[26].

Immunohistochemistry

Retinas were freshly dissected and immediately placed in 10% formalin overnight. Relief cuts were made and the retinas were embedded in 5% agarose. Using a vibratome, 150 μm transverse sections were cut and the sections were floated in PBS. After blocking in 1% bovine serum albumin, 0.5% Triton X-100, and 2% normal donkey serum for 2–3 hours, sections were incubated in primary antibody overnight at 4° C. After washing in PBS, secondary antibodies were applied at room temperature for 1 hour. Sections were again washed and then mounted for confocal microscopy (LSM710, Carl Zeiss). Antibodies were as follows: 3R10 mouse anti-RS1[7] (gift of Professor Robert Molday, 1:5); rabbit anti-GS (Sigma, 1:1000); rabbit anti-synaptophysin (abcam, 1:1000).

Intravitreal injections

C57BL/6J or *Rs1h*−/− mice on a C57BL/6 background[7] were used for all experiments, which were conducted according to the ARVO Statement for the Use of Animals and the

guidelines of the Office of Laboratory Animal Care at the University of California Berkeley, CA. P14 or P30 mice were anesthetized with ketamine (72 mg/kg) and xylazine (64 mg/kg) by intraperitoneal injection. An ultrafine 30 1/2-gauge disposable needle was then passed through the sclera, at the equator and posterior to the limbus, into the vitreous cavity. One μL of AAV with a titer of 5E+13 vg/mL was injected into the vitreous cavity with direct observation of the needle directly above the optic nerve head. Contralateral control eyes received vectors carrying the gene encoding GFP.

Western blot

Three retinas for each condition were pooled. Retinas were removed from the eye cup in cold PBS, sonicated in buffer with proteinase inhibitor cocktail and pooled. Protein concentration was measured using a BCA kit and normalized. Protein was run on a 4–20% Tris-HCL gradient gel. Protein was transferred to a PVDF membrane, and blocked in 5% milk for 2 hours. The membrane was then washed 2X 5 minutes in PBST, and incubated in primary antibodies overnight at RT: 3R10 mouse anti-RS1 (1:50); anti-B-actin (Abcam, 1:2000) PNA (Molecular probes, 1:50). Secondary antibodies conjugated to alkaline phosphatase were applied for 2 hours at RT before washing and visualization using NBT/BCIP (Roche).

Electroretinograms

Mice were dark-adapted for 2 hours and then anesthetized, followed by pupil dilation. Mice were placed on a 37°C heated pad and contact lenses were positioned on the cornea of both eyes. A reference electrode connected to a splitter was inserted into the forehead and a ground electrode was inserted in the tail. For scotopic conditions electroretinograms were recorded (Espion E2 ERG system; Diagnosys LLC, Littleton, MA) in response to six light flash intensities ranging from −3 to 1 log cd × s/m^2 on a dark background. Each stimulus was presented in series of three. For photopic ERGs the animal was exposed to a rod saturating background for 5 minutes. Stimuli ranging from −0.9 to 1.4 log cd × s/m^2 were presented 20 times on a lighted background. Stimulus intensity and timing were computer controlled. Data were analyzed with MatLab (v7.7; Mathworks, Natick, MA). ERG amplitudes were compared using a one-way ANOVA with posthoc Tukey's multiple comparison on Graphpad Prism Software.

High-resolution spectral domain optical coherence tomography

Histological imaging was performed using an 840nm SDOIS OCT system (Bioptigen, Durham, North Carolina) including an 840nm SDOIS Engine with 93nm bandwidth internal source providing < 3.0um resolution in tissue. Retinal thickness, ONL and inner and outer segment thickness measurements were gathered and analysis done using InVivoVue software. Mice were anesthetized and the pupils dilated with atropine before imaging. Images of retinal cross sections were averaged from 8 contiguous slices.

Primary Müller culture

Mouse retinas were dissociated with 0.25% trypsin followed by trituration, and then cultured in DMEM containing 20% FBS, 2mM L-glutamine with antibiotics (100 U penicillin/mL

and 100 ug/mL streptomycin). After 5 days in culture, retinal neurons no longer survive, leaving only Müller cells. Müller glia were then passaged and grown to 80% confluency before infecting in culture with ShH10-CAG-RS1 (MOI of 20,000). Conditioned media and cultured cells were then collected for western blotting.

Acknowledgments

The authors thank Robert Molday for providing the 3R10 anti-RS1 antibody. We thank Bernhardt Weber and Bill Hauswirth for supplying the mouse model of XLRS. We thank Günter Niemeyer, Greg Nielsen, and Matt LaVail for valuable advice on ERG recordings. Tim Day assisted with plasmid cloning. Jonathan Jui helped with immunohistochemistry. This work was supported by funding from the NIH and FFB.

References

1. Sauer CG, Gehrig A, Warneke-Wittstock R, Marquardt A, Ewing CC, Gibson A, et al. Positional cloning of the gene associated with X-linked juvenile retinoschisis. Nat Genet. 1997; 17:164–70. [PubMed: 9326935]
2. George ND, Yates JR, Moore AT. X linked retinoschisis. The British journal of …. 1995
3. Sikkink SK, Biswas S, Parry NRA, Stanga PE, Trump D. X-linked retinoschisis: an update. J Med Genet. 2007; 44:225–32. [PubMed: 17172462]
4. Forsius HH, Krause UU, Helve JJ, Vuopala VV, Mustonen EE, Vainio-Mattila BB, et al. Visual acuity in 183 cases of X-chromosomal retinoschisis. Can J Ophthalmol. 1973; 8:385–93. [PubMed: 4742888]
5. Vijayasarathy C, Takada Y, Zeng Y, Bush RA, Sieving PA. Retinoschisin is a peripheral membrane protein with affinity for anionic phospholipids and affected by divalent cations. Investigative Ophthalmology & Visual Science. 2007; 48:991–1000. [PubMed: 17325137]
6. Molday LL, Wu WWH, Molday RS. Retinoschisin (RS1), the protein encoded by the X-linked retinoschisis gene, is anchored to the surface of retinal photoreceptor and bipolar cells through its interactions with a Na/K ATPase-SARM1 complex. J Biol Chem. 2007; 282:32792–801. [PubMed: 17804407]
7. Weber BHF, Schrewe H, Molday LL, Gehrig A, White KL, Seeliger MW, et al. Inactivation of the murine X-linked juvenile retinoschisis gene, Rs1h, suggests a role of retinoschisin in retinal cell layer organization and synaptic structure. Proc Natl Acad Sci U S A. 2002; 99:6222–7. [PubMed: 11983912]
8. Gehrig A, Janssen A, Horling F, Grimm C, Weber BHF. The role of caspases in photoreceptor cell death of the retinoschisin-deficient mouse. Cytogenet Genome Res. 2006; 115:35–44. [PubMed: 16974082]
9. Dalkara D, Byrne LC, Klimczak RR, Visel M, Yin L, Merigan WH, et al. In vivo-directed evolution of a new adeno-associated virus for therapeutic outer retinal gene delivery from the vitreous. Science Translational Medicine. 2013; 5:189ra76.
10. Park TK, Wu Z, Kjellstrom S, Zeng Y, Bush RA, Sieving PA, et al. Intravitreal delivery of AAV8 retinoschisin results in cell type-specific gene expression and retinal rescue in the Rs1-KO mouse. Gene Ther. 2009; 16:916–26. [PubMed: 19458650]
11. Takada Y, Vijayasarathy C, Zeng Y, Kjellstrom S, Bush RA, Sieving PA. Synaptic pathology in retinoschisis knockout (Rs1-/y) mouse retina and modification by rAAV-Rs1 gene delivery. Investigative Ophthalmology & Visual Science. 2008; 49:3677–86. [PubMed: 18660429]
12. Janssen A, Min SH, Molday LL, Tanimoto N, Seeliger MW, Hauswirth WW, et al. Effect of late-stage therapy on disease progression in AAV-mediated rescue of photoreceptor cells in the retinoschisin-deficient mouse. Mol Ther. 2008; 16:1010–7. [PubMed: 18388913]
13. Kjellstrom S, Bush RA, Zeng Y, Takada Y, Sieving PA. Retinoschisin gene therapy and natural history in the Rs1h-KO mouse: long-term rescue from retinal degeneration. Investigative Ophthalmology & Visual Science. 2007; 48:3837–45. [PubMed: 17652759]

14. Molday LL, Min S-H, Seeliger MW, Wu WWH, Dinculescu A, Timmers AM, et al. Disease mechanisms and gene therapy in a mouse model for X-linked retinoschisis. Adv Exp Med Biol. 2006; 572:283–9. [PubMed: 17249585]
15. Min SH, Molday LL, Seeliger MW, Dinculescu A, Timmers AM, Janssen A, et al. Prolonged recovery of retinal structure/function after gene therapy in an Rs1h-deficient mouse model of x-linked juvenile retinoschisis. Molecular Therapy. 2005; 12:644–51. [PubMed: 16027044]
16. Zeng Y, Takada Y, Kjellstrom S, Hiriyanna K, Tanikawa A, Wawrousek E, et al. RS-1 Gene Delivery to an Adult Rs1h Knockout Mouse Model Restores ERG b-Wave with Reversal of the Electronegative Waveform of X-Linked Retinoschisis. Investigative Ophthalmology & Visual Science. 2004; 45:3279–85. [PubMed: 15326152]
17. Klimczak RR, Koerber JT, Dalkara D, Flannery JG, Schaffer DV. A novel adeno-associated viral variant for efficient and selective intravitreal transduction of rat Müller cells. PLoS ONE. 2009; 4:e7467. [PubMed: 19826483]
18. Koerber JT, Klimczak R, Jang J-H, Dalkara D, Flannery JG, Schaffer DV. Molecular evolution of adeno-associated virus for enhanced glial gene delivery. Mol Ther. 2009; 17:2088–95. [PubMed: 19672246]
19. Reid SNM, Yamashita C, Farber DB. Retinoschisin, a photoreceptor-secreted protein, and its interaction with bipolar and muller cells. Journal of Neuroscience. 2003; 23:6030–40. [PubMed: 12853421]
20. Reid SNM, Farber DB. Glial transcytosis of a photoreceptor-secreted signaling protein, retinoschisin. Glia. 2005; 49:397–406. [PubMed: 15538749]
21. Friedrich U, Stöhr H, Hilfinger D, Loenhardt T, Schachner M, Langmann T, et al. The Na/K-ATPase is obligatory for membrane anchorage of retinoschisin, the protein involved in the pathogenesis of X-linked juvenile retinoschisis. Human Molecular Genetics. 2011; 20:1132–42. [PubMed: 21196491]
22. Wetzel RK, Arystarkhova E, Sweadner KJ. Cellular and subcellular specification of Na, K-ATPase alpha and beta isoforms in the postnatal development of mouse retina. Journal of Neuroscience. 1999; 19:9878–89. [PubMed: 10559397]
23. Takada Y, Fariss RN, Tanikawa A, Zeng Y, Carper D, Bush R, et al. A retinal neuronal developmental wave of retinoschisin expression begins in ganglion cells during layer formation. Investigative Ophthalmology & Visual Science. 2004; 45:3302–12. [PubMed: 15326155]
24. Stieger K, Colle M-A, Dubreil L, Mendes-Madeira A, Weber M, Le Meur G, et al. Subretinal delivery of recombinant AAV serotype 8 vector in dogs results in gene transfer to neurons in the brain. Mol Ther. 2008; 16:916–23. [PubMed: 18388922]
25. Grieger JC, Choi VW, Samulski RJ. Production and characterization of adeno-associated viral vectors. Nat Protoc. 2006; 1:1412–28. [PubMed: 17406430]
26. Aurnhammer C, Haase M, Muether N, Hausl M, Rauschhuber C, Huber I, et al. Universal real-time PCR for the detection and quantification of adeno-associated virus serotype 2-derived inverted terminal repeat sequences. Hum Gene Ther Methods. 2012; 23:18–28. [PubMed: 22428977]

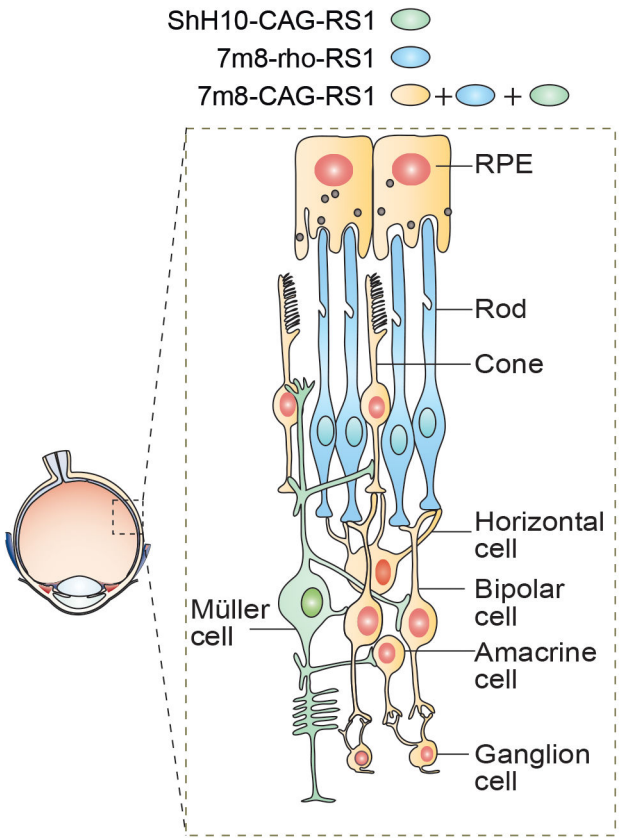

Figure 1. Illustration of experimental plan

Three vectors were used to deliver RS1 to specific populations of retinal cells following intravitreal injection. ShH10 targets Müller glia (in green), which contact all retinal neurons and span the retina from the inner limiting membrane to the outer limiting membrane. 7m8 with a rhodopsin promoter specifically expresses in photoreceptors (in blue). 7m8 with a ubiquitous CAG promoter penetrates to the outer retina from the vitreous and infects all retinal cell types (orange), including ganglion cells, photoreceptors and Müller glia.

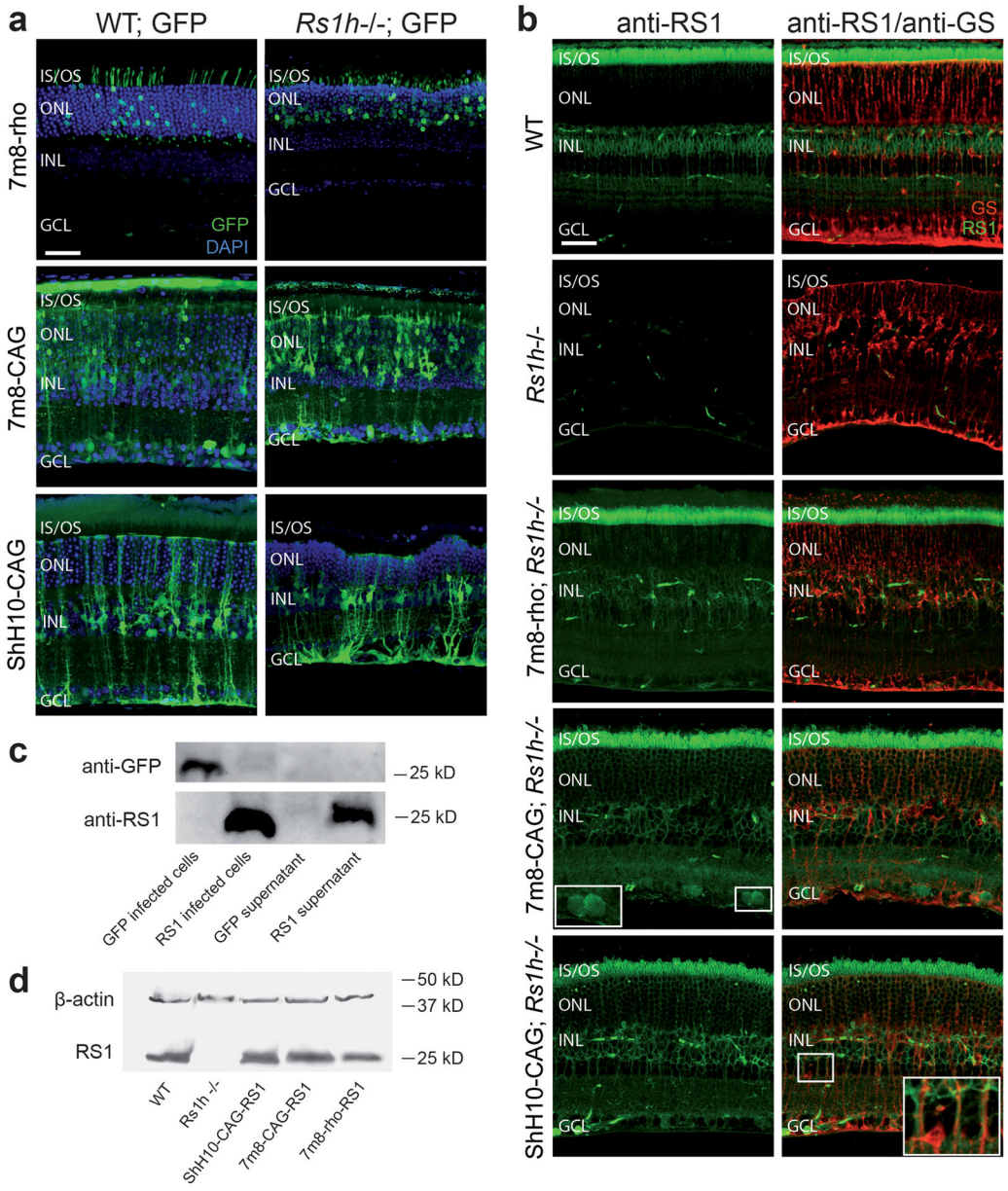

Figure 2. Characterization of viral vectors

(a) GFP expression in WT and *Rs1h*−/− retinas four months after intravitreal injection of viral vectors shows the cell types targeted. 7m8-rho-GFP leads to expression specifically in photoreceptors. 7m8-CAG-GFP leads to expression in all retinal layers. ShH10-CAG-GFP specifically expresses in Müller glia. Blue is DAPI labeled nuclei. Green is native GFP expression. (b) Expression of RS1 4 months after intravitreal injection of the three vectors. First row: Labeling of retinoschisin in the WT retina shows localization in inner segments of photoreceptors, bipolar cells and the photoreceptor-bipolar cell synapse, while *Rs1h*−/− retinas (second row) are devoid of the protein. Third row: 7m8-rho-RS1 injection in Rs1h−/− mice leads to strong expression of the protein with localization of the protein like in the WT retina. Fourth row: 7m8-CAG-RS1 leads to similar levels of protein expression in inner

segments and the inner plexiform layer, although the protein is also expressed from Müller cells and ganglion cells. Inset shows magnification of RS1 expression in ganglion cell bodies. Fifth row: ShH10-CAG-RS1 injection in *Rs1h*−/− mice leads to RS1 protein localization in all retinal layers, including inner segments of photoreceptors, although the staining in photoreceptors was less strong than with the 7m8 vectors. Inset shows detail of RS1 staining on bipolar cell processes running parallel to Müller glia. Red is labeling of the Müller cell marker glutamine synthetase (GS). Green is labeling of RS1. (c) Mouse Müller cells infected with ShH10-RS1 secrete RS1. Primary Müller cell cultures were infected with ShH10-GFP or ShH10-RS1. GFP was present only in cell lysate from cells infected with ShH10-GFP, but not in culture media or in cells infected with ShH10-RS1 (top row). RS1, in contrast, was secreted and was found in both cell lysate and culture media (bottom row). (d) A western blot from retinas injected with ShH10, 7m8-CAG or 7m8-rho shows that levels of expression are similar to WT following treatment with all three vectors. IS/OS = inner and outer segments; ONL=outer nuclear layer; INL = inner nuclear layer; GCL = ganglion cell layer.

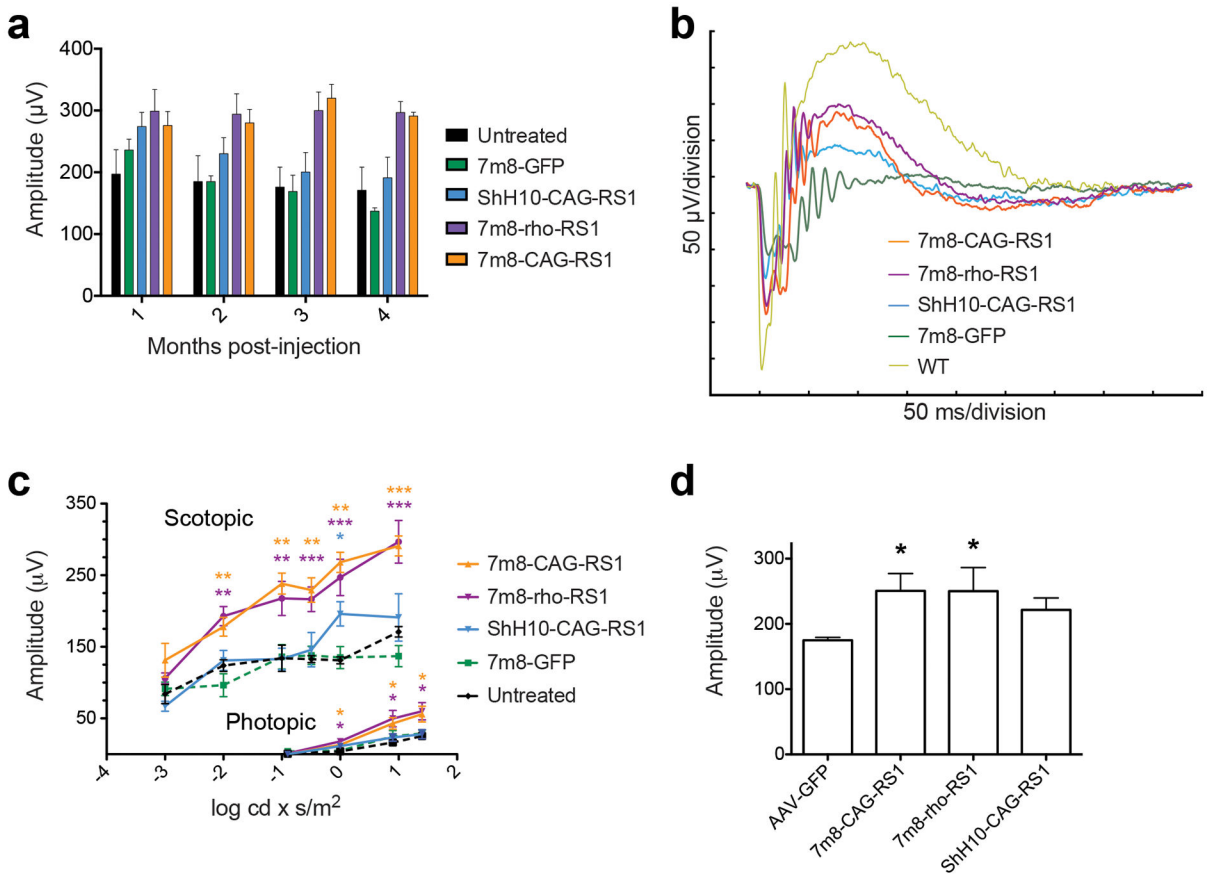

Figure 3. Time-course of functional rescue

(a) The amplitude of the b-wave resulting from a high intensity (1 log cd x s/m^2) stimulus was recorded on a monthly basis beginning one month after P14injection for each condition (ShH10-CAG-RS1 n=5, 7m8-rho-RS1 n=8, 7m8-CAG-RS1 n=5. 7m8-rho-GFP n=8, untreated n=8). In eyes injected with ShH10-CAG-RS1, b-wave amplitudes were slightly higher than control eyes for all time points measured, although the amplitude decreased over time. 7m8-CAG-RS1 and 7m8-rho-RS1 injected eyes were similar to each other and had markedly increased amplitudes compared to contralateral control GFP-injected eyes. (b) Representative ERG traces from all injected conditions, four months post-injection, illustrate a larger amplitude in 7m8-CAG or 7m8-rho-RS1 injected eyes compared to 7m8-GFP-injected eyes. ShH10-CAG-RS1 injected eyes had a slightly increased amplitude. (c) The amplitude of the ERG b-wave recorded four months after injection under a range of light intensities and under scotopic (upper traces) and photopic (lower traces) conditions. 7m8-CAG and 7m8-rho injected eyes had increased amplitudes at all light intensities, while ShH10-RS1-injected eyes were only slightly increased, mostly at higher light intensities greater than 0 log cd x s/m^2. Asterisks above the plot indicate the statistical significance of the difference between treated and GFP-injected eyes for ShH10-CAG-RS1 (blue asterisks) 7m8-CAG-RS1 (orange asterisks) or 7m8-rho-RS1 (purple asterisks). (d) Average b-wave amplitudes of mice injected at P30 and tested four months after injection. Rescue with 7m8-CAG and 7m8-rho is similar, while the amplitudes of mice injected with ShH10 are

increased compared to control eyes but lower than 7m8 (n=5 for all groups). Error bars are mean±SD. * = P<0.05; ** = P<0.01; ** = P<0.001.

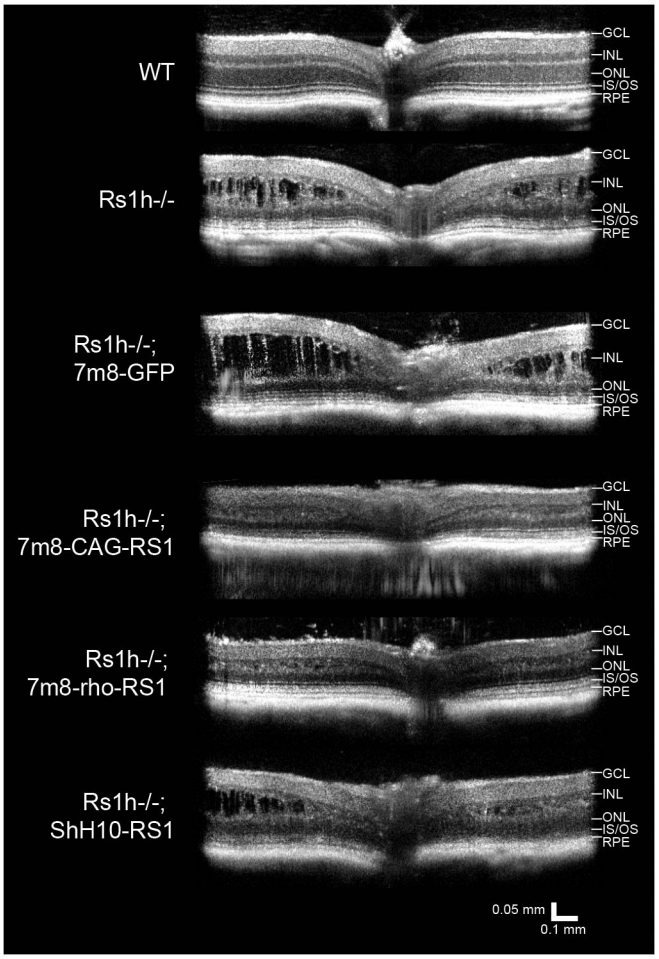

Figure 4. In vivo imaging of treated eyes 4 months after injection

Imaging of treated retinas showed that compared to WT mice, *Rs1h*−/− retinas were marked by the presence of large cavities in the superior and inferior retina. Similarly, 7m8-GFP treated eyes were highly disorganized, with large cavities. In comparison, 7m8-CAG-RS1 and 7m8-rho-RS1 retinas had fewer and smaller holes. ShH10-RS1-injected eyes were also marked by the presence of cavities. For each treatment group n=5 animals were imaged.

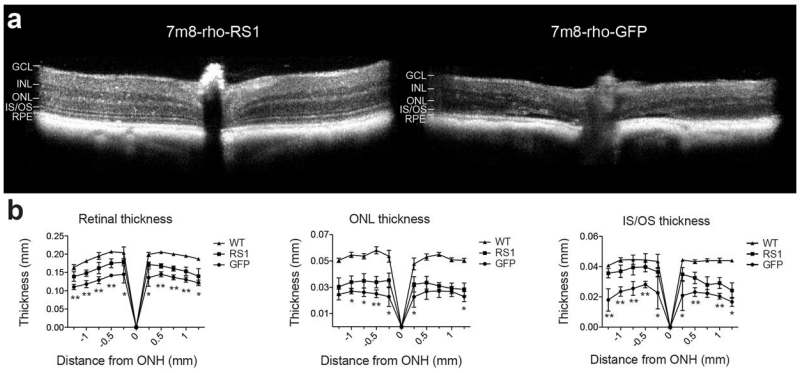

Figure 5. In vivo imaging of long-term structural rescue

(a) SD-OCT images of 7m8-rho-RS1 or 7m8-rho-GFP treated retinas 10 months post-injection showed improved retinal structure in 7m8-treated eyes. (b) Measurements of retinal thickness, ONL thickness and inner and outer segment thickness showed increased thickness in 7m8-rho-RS1 treated retinas in superior and inferior portions of the retina. Asterisks indicate statistical significance of the difference between treated and untreated eyes at the eccentricity measured as determined by a paired 2-tailed Student's t-test. * = $P<0.05$, ** = $P<0.01$. n=5 for each condition. Error bars are mean±SD.

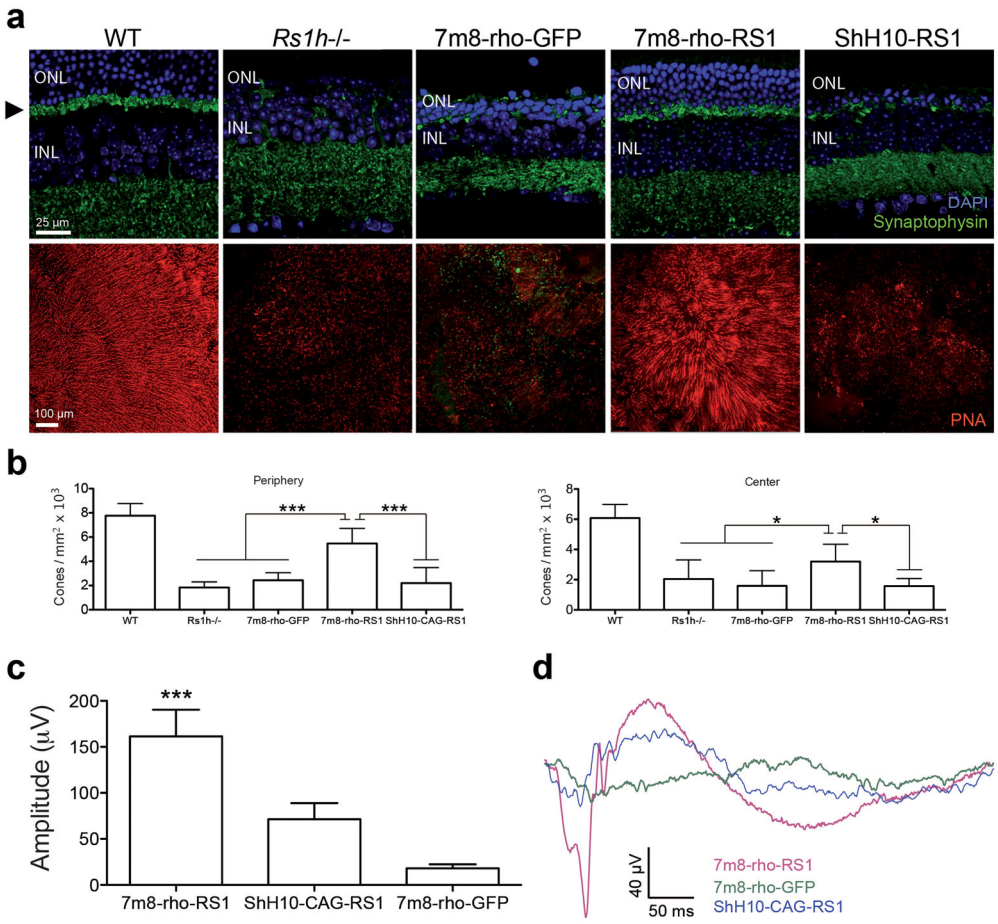

Figure 6. Long-term structural and functional rescue

(a) Retinas collected from mice 15 months post-injection and labeled with anti-synaptophysin antibodies showed that the structure of the photoreceptor-bipolar cell synapse was maintained in mice injected with 7m8-rho-RS1, and looked more like WT compared to untreated *Rs1h*−/− eyes or control 7m8-GFP-injected eyes. ShH10-RS1 injected eyes also showed synaptic deterioration. PNA labeling, which labels cones, showed that the population of structurally intact cones in *Rs1h*−/− mouse retinas is nearly eliminated by 15 months after birth. Mouse eyes treated with 7m8-rho-RS1 showed a much improved cone histology, with widespread labeling of surviving cones. However, at this time point ShH10-injected eyes showed no cone preservation compared to control eyes. (b) Quantification of cone labeling in peripheral and central retina showed that 7m8-rho-RS1 treated eyes had significantly greater numbers of cones compared to untreated or control eyes (n=5 for each group). ShH10-treated eyes (n=5) had similar numbers of cones compared to untreated eyes. (c) ERGs recorded 15 months after injection showed preservation of the b-wave in 7m8-rho-RS1-treated eyes compared to 7m8-rho-GFP-treated eyes or ShH10-CAG-RS1-treated eyes (n=5 per group). (d) Representative ERG traces show that 7m8-rho-RS1 treated eyes had a more normal wave form and a higher amplitude of the a- and b-wave compared to ShH10 or contralateral control eyes. Error bars are mean±SD. *** = P<0.001, * = P<0.05.